HHS Public Access

Author manuscript

J Am Chem Soc. Author manuscript; available in PMC 2019 December 26.

Published in final edited form as:

J Am Chem Soc. 2018 December 26; 140(51): 17830–17834. doi:10.1021/jacs.8b09740.

Visible-Light-Driven Conversion of CO_2 to CH_4 with an Organic Sensitizer and an Iron Porphyrin Catalyst

Heng Rao[†], **Chern-Hooi Lim**[‡], **Julien Bonin**[†], **Garret M. Miyake**[*,‡], and **Marc Robert**[*,†]

[†]Université Paris Diderot, Sorbonne Paris Cité, Laboratoire d'Electrochimie Moléculaire, UMR 7591 CNRS, 15 rue Jean-Antoine de Baïf, F-75205 Paris Cedex 13, France

[‡]Department of Chemistry, Colorado State University, Fort Collins, Colorado 80523, United States

Abstract

Using a phenoxazine-based organic photosensitizer and an iron porphyrin molecular catalyst, we demonstrated photochemical reduction of CO_2 to CO and CH_4 with turnover numbers (TONs) of 149 and 29, respectively, under visible-light irradiation ($\lambda > 435$ nm) with a tertiary amine as sacrificial electron donor. This work is the first example of a molecular system using an earth-abundant metal catalyst and an organic dye to effect complete $8e^-/8H^+$ reduction of CO_2 to CH_4, as opposed to typical $2e^-/2H^+$ products of CO or formic acid. The catalytic system continuously produced methane even after prolonged irradiation up to 4 days. Using CO as the feedstock, the same reactive system was able to produce CH_4 with 85% selectivity, 80 TON and a quantum yield of 0.47%. The redox properties of the organic photosensitizer and acidity of the proton source were shown to play a key role in driving the $8e^-/8H^+$ processes.

In the quest of solar fuels production from CO_2, the ability to effect multielectron and -proton transfer processes with good selectivity remains a daunting challenge.[1–6] Molecular catalysts offer good reactivity and such systems have been shown predominantly to produce the $2e^-/2H^+$ reduction products of CO (carbon monoxide) or HCOOH (formic acid).[7–9] In these $2e^-/2H^+$ reduction systems, both electrochemical and photochemical approaches have been successfully developed using earth-abundant metal catalysts and sometimes metal free sensitizers in the case of photostimulated reactions.[10] Recently, some of us were able to achieve $8e^-/8H^+$ reduction of CO_2 to CH_4 (methane) by employing a dual catalytic approach that combined an iron porphyrin catalyst (**Fe-*p*-TMA,** Scheme 1) with an iridium-based photosensitizer *fac*-Ir(ppy)$_3$ (*fac*-tris[2-phenylpyridinato-C^2,*N*]iridium(III)).[11] To date, it was the only molecular based system that could achieve such a complete $8e^-/8H^+$ reduction process. Comparatively, heterogeneous systems have shown more advanced progress for CO_2-to-CH_4 reduction. Semiconductive solid materials doped with cocatalysts have been recently developed for CH_4 production at ambient temperature and pressure, with hydrocarbon production rate up to a few hundred μmol g_{cat}^{-1} h^{-1}, [12–18] and sometimes with

[*]**Corresponding Authors** robert@univ-paris-diderot.fr, garret.miyake@colostate.edu.

Supporting Information

The Supporting Information is available free of charge on the ACS Publications website at DOI:10.1021/jacs.8b09740.

Materials preparation, methods, photochemical and photophysical data, apparent quantum yield estimation (PDF)

The authors declare no competing financial interest.

excellent selectivity.[19] In the latter example, TiO_2 was used as a photocatalyst with Pd_7Cu_1 alloy as a nano cocatalyst to yield CH_4 with a high selectivity of 96% at a rate of 19.6 μmol g_{cat}^{-1} h^{-1}. Like their molecular counterpart, these heterogeneous systems principally employ noble metals to boost reactivity.

Noble-metal-based photosensitizers, exemplified by polypyridyl ruthenium(II) and iridium(III) compounds,[20,21] are commonly used in photoredox catalysis[22] and other important energy conversion processes. Despite their proven performance in numerous light-driven reactions, these noble-metal compounds pose long-term supply and cost issues that their replacement by organic photosensitizers is of significant interest.[23] In this context, a few of us have recently developed organic photosensitizers based on the dihydrophenazine (**Phen1**,[24] 5,10-di(2-naphthyl)−5,10-dihydrophenazine) and phenoxazine[25,26] (**Phen2**, 3,7-di(4-biphenyl)-1-naphthalene-10-phenoxazine) motifs (Scheme 1). These organic chromophores exhibit photon absorption in the visible light spectrum, redox reversibility, good triplet quantum yields [e.g., 2% (**Phen1**) and 90% (**Phen2**)], and long triplet lifetimes [ca. 4.3 μs (**Phen1**) and 480 μs (**Phen2**)].[27] In particular, **Phen1** and **Phen2** were specifically engineered as strong excited-state electron donors with highly negative excited state reduction potentials for oxidative quenching applications. The triplet excited state reduction potential values of **Phen1** and **Phen2** are $E^0(^2\mathbf{Phen1}^{\bullet+}/^3\mathbf{Phen1}^*)$ = −2.09 V vs Fc^+/Fc and $E^0(^2\mathbf{Phen2}^{\bullet+}/^3\mathbf{Phen2}^*)$ = −2.20 V vs Fc^+/Fc, respectively (values in N,N-dimethylacetamide as solvent); notably, these values closely match the $E^0(\mathrm{Ir(IV)}/^3\mathrm{Ir(III)}^*)$ = −2.13 V vs Fc^+/Fc for $Ir(ppy)_3$, which were successfully employed for the photochemical reduction of CO_2 to CH_4. Given these properties, we hypothesized that **Phen1** or **Phen2** could directly replace $Ir(ppy)_3$ in the light-driven tandem catalysis with **Fe-*p*-TMA** for CO_2 reduction. Herein, we report a noble metal free molecular system for visible light-driven $8e^-/8H^+$ reduction of CO_2 to CH_4 with an organic photosensitizer (**Phen2**) and an earth-abundant iron porphyrin catalyst (**Fe-*p*-TMA**). Such a premiere is expected to advance the field of photochemical CO_2 reduction and contribute to the mechanistic understanding of multielectron and -proton transfer processes in CO_2 reduction.

In Figure 1 (open symbols), under visible-light irradiation (λ > 435 nm), we monitored the evolution of products as a function of time for a CO_2-saturated DMF (*N,N*'-dimethyl-formamide) solution containing 10 μM **Fe-*p*-TMA**, 1 mM **Phen2**, and 0.1 M TEA (triethylamine) acting as a sacrificial electron donor (SD). Large excess of **Phen2** was used to ensure a strong light absorption as well as an efficient bimolecular subsequent reaction with the catalyst. Gratifyingly, we observed CH_4 production, albeit in moderate yield (TON of 8 after 47 h), alongside with the formation of H_2 (dihydrogen) and CO (TON of 8 and 50, respectively, Table 1 entry 1); note that the TON is defined as the mol number of product divided by the mol number of **Fe-*p*-TMA**. No other products such as formic acid, formaldehyde or methanol were detected. Importantly, the omission of any single reactive component (Fe catalyst, organic sensitizer, SD, CO_2, or light) produced no CH_4 product. Further, we found that with the addition of 0.1 M 2,2,2-trifluoroethanol (TFE) as an external acid, the production of CO and CH_4 was noticeably improved (TON of 71 and 14, respectively, see Figure 1 and Table 1 entry 2), whereas the production of H_2 remains almost unchanged (compare entries 1 and 2 in Table 1). GC/MS experiments performed under a

$^{13}CO_2$ atmosphere confirmed that the produced CH_4 originated from CO_2 (Figure S1). Moreover, long-term irradiation (over 100 h) led to a TON in CH_4 of 29 and CO of 140 (Figure 2 and Table 1 entry 3). Catalytic selectivity for methane is 15%. The stability of the system was followed by UV–vis absorption spectroscopy over the entire irradiation course (Figure S3) and it showed no major **Fe-*p*-TMA** or **Phen2** degradation. We have previously demonstrated that the dual catalysis employing **Fe-*p*-TMA** and $Ir(ppy)_3$ could also use CO as a starting substrate.[11] The rationale was that CO is an intermediary species toward the highly reduced CH_4 product. In Figure 3, using **Phen2** as a photosensitizer in a CO-saturated solution, we observed the formation of CH_4 with a TON of 10 (Table 1 entry 4) and a selectivity of 30%, while H_2 was formed as the major product. The addition of 0.1 M TFE, however, significantly boosted CH_4 formation with a TON of 45 (Table 1 entry 5) and 87% selectivity upon 47 h of irradiation. The nature of the SD (Table 1, entries 5 to 8) had only minor effects on CH_4 production, e.g. similar results were obtained with TEA, DIPEA (*N,N*-diisopropylethylamine) and BIH (1,3-dimethyl-2-phenyl-2,3-dihydro-1H-benzo[*d*]imidazole), while TEOA (triethanolamine) gave lower CH_4 production. GC/MS experiments performed under a ^{13}CO atmosphere again confirmed that the produced CH_4 was originated from CO (Figure S2). On the contrary, the types of acids used had a marked influence on CH_4 yield (Figure 3). Water, being a weaker acid than TFE, resulted in a much lower amount of CH_4 even with concentration up to 0.5 M (Table 1, entries 12 and 13). Conversely, the addition of 0.1 M PhOH (phenol, Table 1 entry 14), which is a stronger proton donor than TFE, resulted in forming H_2 as a major product and a decrease in CH_4 production. Further, the use of higher concentrations of TFE (greater than 0.1 M) reversed the catalytic selectivity toward H_2 formation (Table 1 entries 10 and 11). Thus, these results showed that 0.1 M TFE provided proper acidity and concentration to maximize CH_4 production and suppress H_2 evolution (see below for a more detailed mechanistic discussion).

By employing 0.1 M TFE in a CO-saturated DMF solution irradiated for 102 h, we were able to produce CH_4 in 80 TON and 85% selectivity (Table 1, entry 9). The corresponding quantum yield is 0.47% based on the chemical actinometer method.[28] As a comparison, the noble metal $Ir(ppy)_3$ catalyzed CH_4 production in 159 TON, 81% selectivity and 0.18% quantum yield under similar reaction conditions (with 0.1 M TFE at optimized conditions).[11] We note that the Fe catalyst concentration in the $Ir(ppy)_3$ case was 5 times less as compared to this study, and thus the absolute mol number of CH_4 produced by the catalytic system comprising **Fe-*p*-TMA** + **Phen2** is in fact ~2 times larger. Consequently, given the higher quantum yield and more CH_4 produced, the system employing the organic dye **Phen2** is significantly more efficient. Table 1 summarizes key results from Figure 1, 2 and 3.

Notably, replacing **Phen2** by the less reducing **Phen1** led to the exclusive formation of CO (TON 60, selectivity 90%) and H_2 (TON 6) upon irradiation of a CO_2-saturated solution. However, irradiation of a CO-saturated solution with **Phenl** only furnished H_2 as the detectable product. These results indicate that the slightly lower reducing ability of **Phenl** led to the inability for further reduction beyond CO.

Investigating the mechanism, emission quenching experiments showed efficient quenching between **Fe-*p*-TMA** and the photoexcited **Phen2** (or **Phen2***) with a second order rate

constant of $k_q \approx (1.60 \pm 0.07) \times 10^8\ M^{-1}\ s^{-1}$ (see Figures S4–S6), which supports an oxidative electron transfer from **Phen2*** to **Fe-*p*-TMA**. This result is in line with the fact that $E^0(^2\mathbf{Phen2}^{\bullet+}/^3\mathbf{Phen2}^*) = -2.20$ V vs Fc^+/Fc[27] is more negative than all three redox couples related to the Fe porphyrin (Fe^{III}/Fe^{II}, Fe^{II}/Fe^{I} and Fe^{I}/Fe^{0}),[29–31] and thus allowing the generation of potential catalytically active Fe^{II}, Fe^{I} and Fe^0 species upon light irradiation.

Scheme 2 highlights our proposed mechanism. As already observed and demonstrated in our previous electrochemical and photochemical studies, CO_2 first complexes to the triply reduced Fe^0 species (to form $Fe^{II}CO_2$), which upon protonations and elimination of water, generates a $Fe^{II}CO$ intermediate.[29–31] This intermediate has been detected by UV–vis absorption spectroscopy in a previous study.[31] We note that the electron-rich Fe^0 species can react with $2H^+$ to form Fe^{II} and the undesired H_2 byproduct, although it remains a minor pathway in our optimized conditions. It is only for higher concentration of the acid or in the presence of a stronger acid that protonation at the metal (and additionally at the ligand) may outcompete CO_2 insertion and favor H_2 production.[29,30] Note also that a high concentration of Fe^0 active species in solution, which would be obtained upon highly efficient electron transfers from the sensitizer, may also favor H_2 evolution. The $Fe^{II}CO$ intermediate can eliminate the CO product and form Fe^{II}. Alternatively, it may participate in further $6e^-/6H^+$ reductions to produce the ultimate CH_4 product. DFT calculations are in progress to get hints on the reaction pathway from CO to methane and will be reported in due time. Note also that transposing the $8e^-$ catalysis of CO_2 to electrochemical conditions is hampered by the fact that the potential would be set at values negative enough to generate the Fe^0 species that are reacting with CO_2. In the reaction–diffusion layer close to the electrode surface, only Fe^0 and Fe^I are present in sizable amounts, with no Fe^{II} accumulation for further reduction of CO to CH_4.

In conclusion, we have successfully demonstrated the first noble metal free molecular system for visible light-driven $8e^-/8H^+$ reduction of CO_2 to CH_4 employing an organic phenoxazine-based photosensitizer (**Phen2**) and an earth-abundant iron porphyrin catalyst (**Fe-*p*-TMA**) at ambient conditions. In a CO_2-saturated DMF solution, CO (TON of 140) and CH_4 (TON of 29) were produced after 102 h of light irradiation; whereas in a CO-saturated solution, CH_4 was produced with TON of 80, a selectivity of 85% and a quantum yield of 0.47%. Remarkably, **Phen2** was significantly more efficient than Ir(ppy)3, producing ~2 times the amount of CH_4 with ~3 times higher quantum yield under similar reaction conditions. We envision that this work will open up new perspectives toward the development of integrated (photo)-electrochemical catalytic systems where the multielectron and -proton conversion of the CO_2 will be coupled to oxidation of water, biomass or organic compounds for sustainable solar fuels production.

Supplementary Material

Refer to Web version on PubMed Central for supplementary material.

ACKNOWLEDGMENTS

H.R. thanks the China Scholarship Council for his PhD fellowship (CSC student number 201507040033). C.-H.L. acknowledges National Institutes of Health (NIH)'s F32 postdoctoral fellowship support (F32GM122392). G.M.M. acknowledges support by Colorado State University and the National Institute of General Medical Sciences (Award R35GM119702) of the NIH. The content is solely the responsibility of the authors and does not necessarily represent the official views of the NIH. We thank D. Clainquart (Chemistry Department, Université Paris Diderot) for assistance in gas chromatography/mass spectrometry analysis. Partial financial support to M.R. from the Institut Universitaire de France (IUF) is gratefully acknowledged.

REFERENCES

(1). Lewis NS; Nocera DG Powering the planet: Chemical challenges in solar energy utilization. Proc. Natl. Acad. Sci. U. S. A. 2006, 103, 15729–15735. [PubMed: 17043226]

(2). Wenzhen L In Advances in CO_2 Conversion and Utilization; ACS Symposium Series; American Chemical Society: Washington, DC, 2010; Vol. 1056, pp 55–76.

(3). Jhong H-RM; Ma S; Kenis PJ Electrochemical conversion of CO_2 to useful chemicals: current status, remaining challenges, and future opportunities. Curr. Opin. Chem. Eng. 2013, 2, 191–199.

(4). Kamat PV Semiconductor Surface Chemistry as Holy Grail in Photocatalysis and Photovoltaics. Acc. Chem. Res. 2017, 50, 527–531. [PubMed: 28945391]

(5). Dau H; Fujita E; Sun L Artificial photosynthesis: Beyond mimicking nature. ChemSusChem 2017, 10, 4228–4235. [PubMed: 29131535]

(6). Wang F Artificial photosynthetic systems for CO_2 reduction: Progress on higher efficiency with cobalt complexes as catalysts. ChemSusChem 2017, 10, 4393–4402. [PubMed: 29055180]

(7). Benson EE; Kubiak CP; Sathrum AJ; Smieja JM Electrocatalytic and homogeneous approaches to conversion of CO_2 to liquid fuels. Chem. Soc. Rev. 2009, 38, 89–99. [PubMed: 19088968]

(8). Appel AM; Bercaw JE; Bocarsly AB; Dobbek H; DuBois DL; Dupuis M; Ferry JG; Fujita E; Hille R; Kenis PJA; Kerfeld CA; Morris RH; Peden CHF; Portis AR; Ragsdale SW; Rauchfuss TB; Reek JNH; Seefeldt LC; Thauer RK; Waldrop GL Frontiers, opportunities, and challenges in biochemical and chemical catalysis of CO_2 fixation. Chem. Rev. 2013, 113, 6621–6658. [PubMed: 23767781]

(9). Francke R; Schille B; Roemelt M Homogeneously catalyzed electroreduction of carbon dioxide-Methods, mechanisms, and catalysts. Chem. Rev. 2018, 118, 4631–4701. [PubMed: 29319300]

(10). Takeda H; Cometto C; Ishitani O; Robert M Electrons, photons, protons and earth abundant metal complexes for molecular catalysis of CO_2 reduction. ACS Catal 2017, 7, 70–88.

(11). Rao H; Schmidt LC; Bonin J; Robert M Visible-light-driven methane formation from CO_2 with an iron complex. Nature 2017, 548, 74–77. [PubMed: 28723895]

(12). Kim W; Seok T; Choi W Nafion layer-enhanced photosynthetic conversion of CO_2 into hydrocarbons on TiO2 nanoparticles. Energy Environ. Sci. 2012, 5, 6066–6070.

(13). AlOtaibi B; Fan S; Wang D; Ye J; Mi Z Wafer-level artificial photosynthesis for CO_2 reduction into CH_4 and CO using GaN nanowires. ACS Catal. 2015, 5, 5342–5348.

(14). Liu X; Inagaki S; Gong J Heterogeneous molecular systems for photocatalytic CO_2 reduction with water oxidation. Angew. Chem., Int. Ed. 2016, 55, 14924–14950.

(15). Wang Y; Bai X; Qin H; Wang F; Li Y; Li X; Kang S; Zuo Y; Cui L Facile one-step synthesis of hybrid graphitic carbon nitride and carbon composites as high-performance catalysts for CO2 photocatalytic conversion. ACS Appl. Mater. Interfaces 2016, 8, 17212–17219. [PubMed: 27112547]

(16). Yu L; Li G; Zhang X; Ba X; Shi G; Li Y; Wong PK; Yu JC; Yu Y Enhanced activity and stability of carbon-decorated cuprous oxide mesoporous nanorods for CO_2 reduction in artificial photosynthesis. ACS Catal. 2016, 6, 6444–6454.

(17). Wang W-N; An W-J; Ramalingam B; Mukherjee S; Niedzwiedzki DM; Gangopadhyay S; Biswas P Size and structure matter: enhanced CO_2 photoreduction efficiency by size-resolved ultrafine Pt nanoparticles on TiO_2 single crystals. J. Am. Chem. Soc. 2012, 134, 11276–11281. [PubMed: 22694165]

(18). Bae K-L; Kim J; Lim CK; Nam KM; Song H Colloidal zinc oxide-copper(I) oxide nanocatalysts for selective aqueous photocatalytic carbon dioxide conversion into methane. Nat. Commun. 2017, 8, 1156. [PubMed: 29109394]

(19). Long R; Li Y; Liu Y; Chen S; Zheng X; Gao C; He C; Chen N; Qi Z; Song L; Jiang J; Zhu J; Xiong Y Isolation of Cu Atoms in Pd Lattice: Forming Highly Selective Sites for Photocatalytic Conversion of CO_2 to CH_4. J. Am. Chem. Soc. 2017, 139, 4486–4492. [PubMed: 28276680]

(20). Prier CK; Rankic DA; MacMillan DWC Visible light photoredox catalysis with transition metal complexes: applications in organic synthesis. Chem. Rev. 2013, 113, 5322–5363. [PubMed: 23509883]

(21). Koike T; Akita M Visible-light radical reaction designed by Ru- and Ir-based photoredox catalysis. Inorg. Chem. Front. 2014, 1, 562–576.

(22). Arias-Rotondo DM; McCusker JK Visible-light radical reaction designed by Ru- and Ir-based photoredox catalysis. Chem. Soc. Rev. 2016, 45, 5803–5820. [PubMed: 27711624]

(23). Romero NA; Nicewicz DA Organic photoredox catalysis. Chem. Rev. 2016, 116, 10075–10166. [PubMed: 27285582]

(24). Theriot JC; Lim C-H; Yang H; Ryan MD; Musgrave CB; Miyake GM Organocatalyzed atom transfer radical polymerization driven by visible light. Science 2016, 352, 1082–1086. [PubMed: 27033549]

(25). Pearson RM; Lim C-H; McCarthy BG; Musgrave CB; Miyake GM Organocatalyzed atom transfer radical polymerization using *N*-aryl phenoxazines as photoredox catalysts. J. Am. Chem. Soc. 2016, 138, 11399–11407. [PubMed: 27554292]

(26). McCarthy BG; Pearson RM; Lim C-H; Sartor SM; Damrauer NH; Miyake GM Structure—property relationships for tailoring phenoxazines as reducing photoredox catalysts. J. Am. Chem. Soc. 2018, 140, 5088–5101. [PubMed: 29513533]

(27). Du Y; Pearson RM; Lim C-H; Sartor SM; Ryan MD; Yang H; Damrauer NH; Miyake GM Strongly reducing, visible-light organic photoredox catalysts as sustainable alternatives to precious metals. Chem. - Eur. J. 2017, 23, 10962–10968. [PubMed: 28654171]

(28). Alsabeh PG; Rosas-Hernandez A; Barsch E; Junge H; Ludwig R; Beller M Iron-catalyzed photoreduction of carbon dioxide to synthesis gas. Catal. Sci. Technol. 2016, 6, 3623–3630.

(29). Bonin J; Robert M; Routier M Selective and efficient photocatalytic CO_2 reduction to CO using visible light and an iron based homogeneous catalyst. J. Am. Chem. Soc. 2014, 136, 16768–16771. [PubMed: 25396278]

(30). Bonin J; Maurin A; Robert M Molecular catalysis of the electrochemical and photochemical reduction of CO_2 with earth-abundant metal complexes Recent advances. Coord. Chem. Rev. 2017, 334, 184–198.

(31). Rao H; Bonin J; Robert M Non-sensitized selective photochemical reduction of CO_2 to CO under visible light with an iron molecular catalyst. Chem. Commun. 2017, 53, 2830–2833.

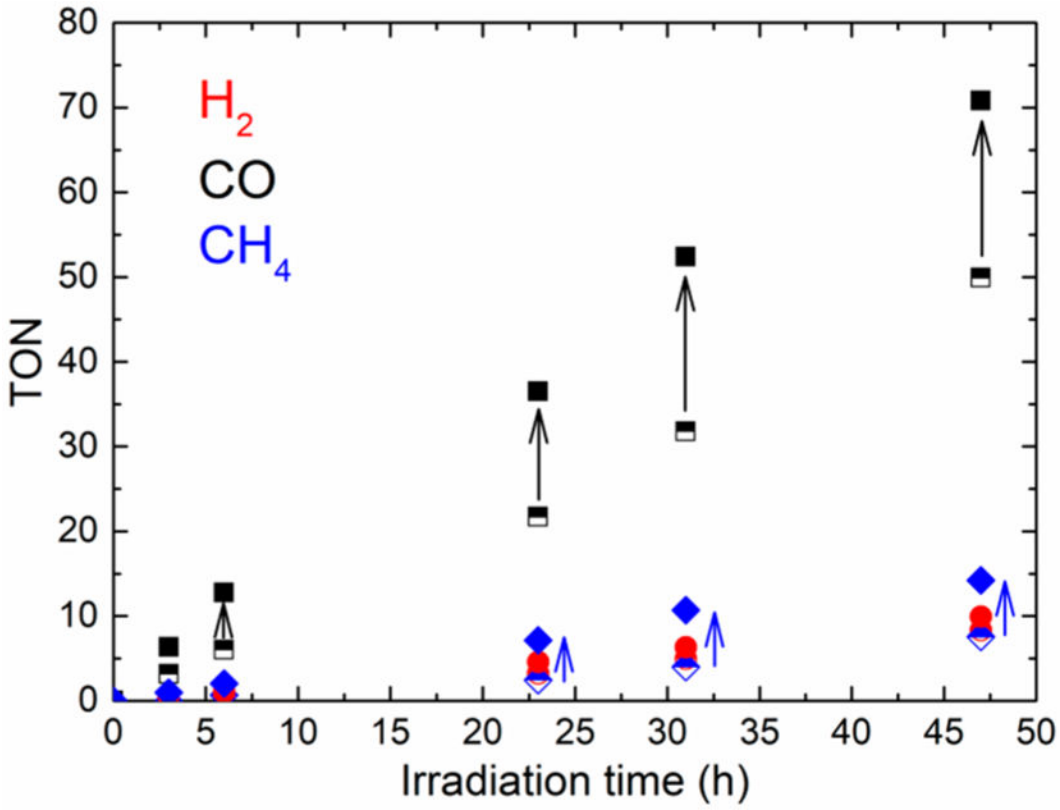

Figure 1.

Generation of CO (black squares), H_2 (red circles) and CH_4 (blue diamonds) with time upon visible light irradiation (λ > 435 nm) of a CO_2-saturated DMF solution containing 10 μM Fe-*p*-TMA, 1 mM **Phen2** and 0.1 M TEA (open symbols); addition of 0.1 M TFE (2,2,2-trifluoroethanol) as an external acid is indicated by "filled symbols". Arrows indicate increase in product formation upon addition of an external acid.

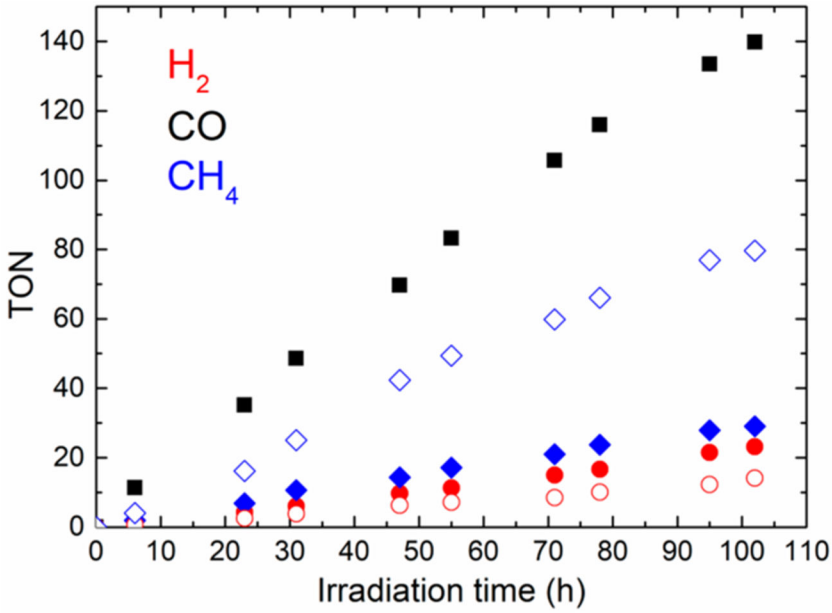

Figure 2.

CO (black squares), H_2 (red circles) and CH_4 (blue diamonds) generation with time upon visible light irradiation (λ > 435 nm) of a CO_2^- (filled symbols) or CO-saturated (open symbols) DMF solution containing 10 μM **Fe-*p*-TMA,** 1 mM **Phen2,** 0.1 M TEA and 0.1 M TFE.

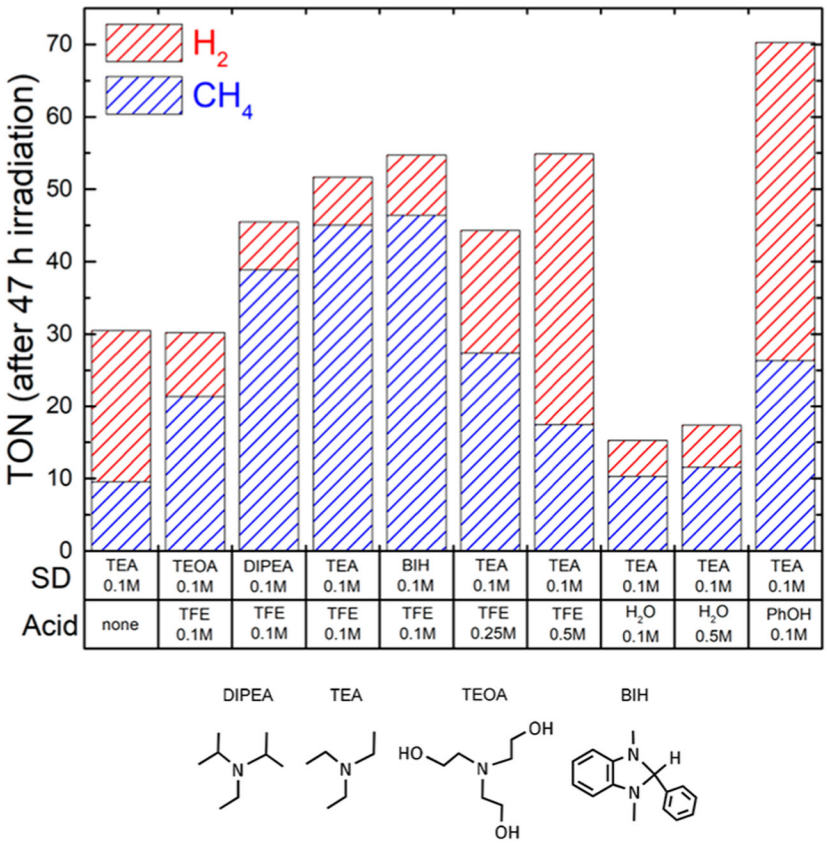

Figure 3.

Catalytic turnovers in H_2 (red) and CH_4 (blue) measured after 47 h of visible light irradiation (>435 nm) of a CO-saturated DMF solution containing 10 μM **Fe-*p*-TMA,** 1 mM **Phen2,** in the presence of various SDs and added acids.

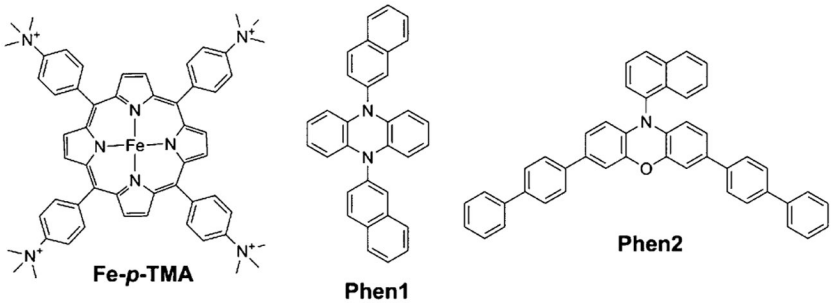

Scheme 1.

Molecular Structures of the Iron Catalyst (Fe-*p*-TMA) and Organic Photosensitizers (Phen1, Phe2) Investigated in This Study

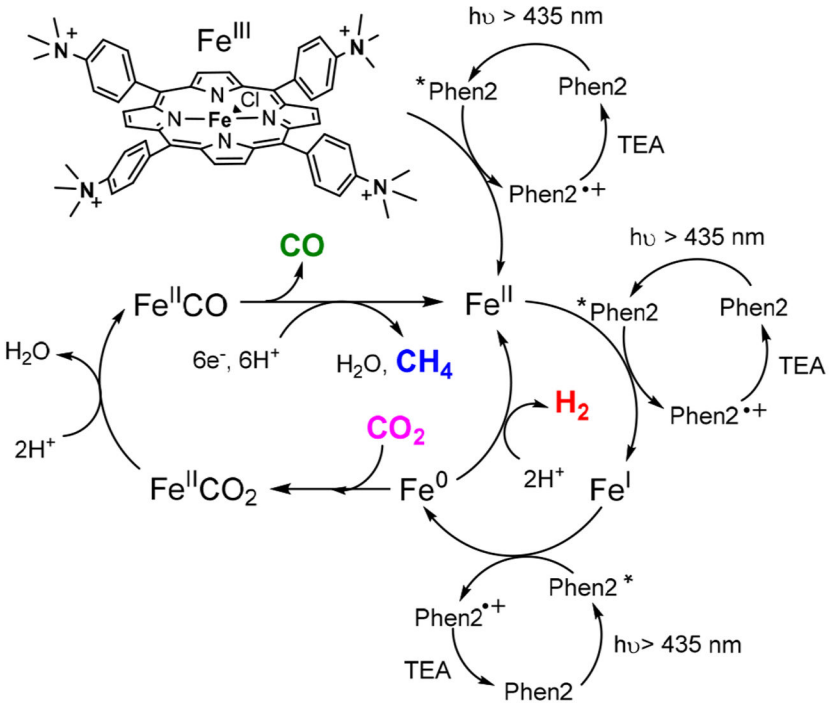

Scheme 2.

Proposed Mechanism for the $8e^{-}$ /$8H^{+}$ Reduction of CO_2 to CH_4 by Tandem Catalysis of Phen2 and Fe-*p*-TMA

Table 1.

Turnover Number (TON) of Gaseous Products Measured after 47 or 102 h[a] of Visible Light (λ > 435 nm) Irradiation of DMF Solution Containing 10 μM Fe-*p*-TMA, 1 mM Phen2 and Various Components (SD, CO_2/CO, acid)

				TON		
entry	**gas**	**SD (M)**	**acid (M)**	**H_2**	**CO**	**CH_4**
1	CO_2	TEA (0.1)	none	8	50	8
2	CO_2	TEA (0.1)	TFE (0.1)	10	71	14
3	CO_2	TEA (0.1)	TFE (0.1)	23[a]	140[a]	29[a]
4	CO	TEA (0.1)	none	21	–	10
5	CO	TEA (0.1)	TFE (0.1)	7	–	45
6	CO	TEOA (0.1)	TFE (0.1)	9	–	21
7	CO	DIPEA (0.1)	TFE (0.1)	7	–	39
8	CO	BIH (0.1)	TFE (0.1)	8	–	46
9	CO	TEA (0.1)	TFE (0.1)	14[a]	–	80[a]
10	CO	TEA (0.1)	TFE (0.25)	17	–	27
11	CO	TEA (0.1)	TFE (0.5)	37	–	17
12	CO	TEA (0.1)	H_2O (0.1)	5	–	10
13	CO	TEA (0.1)	H_2O (0.5)	6	–	12
14	CO	TEA (0.1)	PhOH (0.1)	44	–	26